Personal Identification Technique based on Human Iris Recognition with Wavelet Transform

Wen-Shiung Chen, Kun-Huei Chih, Sheng-Wen Shih* and Chih-Ming Hsieh**

VIP-CCLab., Dept. of Electrical Engineering, National Chi Nan University, Taiwan
*Dept. of Computer Science and Information Engineering, National Chi Nan University, Taiwan
**Dept. of Information Management, Hsiuping Institute of Technology, Taichung, Taiwan

ABSTRACT

This paper presents a biometric recognition system based on the iris of a human eye using wavelet transform. The proposed system includes three modules: image preprocessing, feature extraction, and recognition modules. The feature extraction module adopts the gradient direction (i.e., angle) on wavelet transform as the discriminating texture features. The system encodes the features to generate its iris feature codes using two efficient coding techniques: binary Gray encoding and delta modulation. Experimental results show that the recognition rates up to 95.27%, 95.62%, 96.21%, and 99.05%, respectively, using different coding methods can be achieved.

1. INTRODUCTION

Biometrics [1] refers to automatic identity authentication of a person on a basis of one's unique physiological or behavioral characteristics. To date, many biometric features have been applied to individual authentication. The iris, a kind of physiological feature with genetic independence, contains extremely information-rich physical structure and unique texture pattern, and thus is highly complex enough to be used as a biometric signature. Statistical analysis reveals that irises have an exceptionally high degree-of-freedom up to 266 (fingerprints show about 78) [1], and thus are the most mathematically unique feature of the human body; more unique than fingerprints. Hence, the human iris promises to deliver a high level of uniqueness to authentication applications that other biometrics cannot match.

In 1993 Dougman developed a successful system by using the 2-D Gabor wavelet transform [2]. In this system, the visible texture of a person's iris in a real-time video image is encoded into a compact sequence of multi-scale quadrature 2-D Gabor wavelet coefficients, whose most significant bits consist of a 256-byte "iris code." In 1996, Wildes *et al.* developed a prototype system based on an automated iris recognition that uses a very computationally demanding image registration technique [3]. This system exploits normalized correlation over small tiles within the Laplacian pyramid bands as a goodness of match measure. Boles and Boashash [4] proposed an iris identification system in which zero-crossing of the wavelet transform at various resolution levels is calculated over concentric circles on the iris, and the resulting 1-D signals are compared with the model features using different dissimilarity functions. Ma *et al.* also adopted wavelet multi-resolution analysis based on Gabor filtering for iris feature extraction [5].

2. SYSTEM OVERVIEW AND PRE-PROCESSING

2.1. System Overview

The proposed framework consists of three modules: image pre-processing, feature extraction, and recognition modules (Fig. 1). Since the system is tested on the CASIA iris image database [6], this paper takes no account of the iris image acquisition module. The entire system flow is briefly described as follows. First, the iris image pre-processing (IIP) module employs some image processing algorithms to demarcate the region of interest (i.e., iris zone) from the input image containing an eye. It performs three major tasks including iris localization, iris segmentation and normalization, and enhancement. Next, the iris feature extraction (IFE) module performs a 2-D wavelet transform, computes the gradient direction features, and applies appropriate coding methods on these features to generate the iris feature code. Finally, the iris pattern recognition (IPR) module employs a minimum distance classifier according to Hamming distance or Euclidean distance metric to recognize the iris pattern by comparing the iris code with the enrolled iris codes in the iris code database.
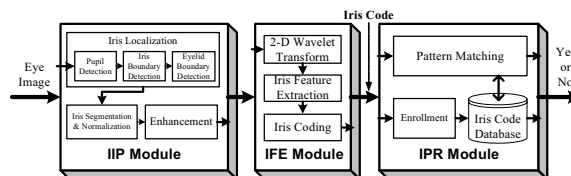

Fig. 1. The proposed iris recognition system.

2.2. Pre-Processing Module

Input image does contain not only useful information from iris zone but also useless data derived from the surrounding eye region. Before extracting the features of an iris, the input image must be pre-processed to localize, segment and enhance the region of interest (i.e., iris zone). The system normalizes the iris region to overcome the problem of a change in camera-to-eye distance and pupil's size variation derived from illumination. Furthermore, the brightness is not uniformly distributed due to non-uniform illumination, the system must be capable of removing the effect and further enhancing the iris image. Hence, the IIP module consists of three units: iris localization, iris segmentation & normalization, and enhancement units (Fig. 2).
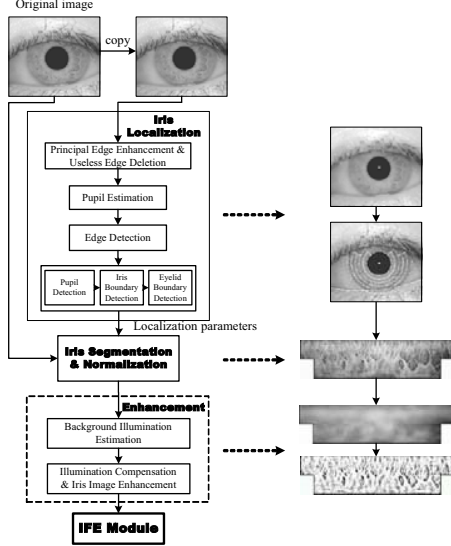
Fig. 2. Pre-processing module.

3. THE PROPOSED IRIS RECOGNITION

3.1. Feature Extraction with Wavelet Transform

Wavelet transform has been widely used to solve the intrinsic redundancies that appear in a multi-scale analysis [7]. The WT components are proportional to the coordinates of the gradient vector of f smoothed by $\overline{\theta}_{2^j}$ ::

$$\begin{pmatrix} W_{2^j}^1 f(u,v) \\ W_{2^j}^2 f(u,v) \end{pmatrix} = 2^j \begin{pmatrix} \frac{\partial}{\partial x}\left(f * \overline{\theta}_{2^j}\right)(u,v) \\ \frac{\partial}{\partial y}\left(f * \overline{\theta}_{2^j}\right)(u,v) \end{pmatrix} = 2^j \vec{\nabla}\left(f * \overline{\theta}_{2^j}\right)(u,v) \quad (1)$$

The modulus of this gradient vector is proportional to the WT modulus

$$M_{2^j} f(u,v) = \sqrt{\left|W_{2^j}^1 f(u,v)\right|^2 + \left|W_{2^j}^2 f(u,v)\right|^2} \cdot \quad (2)$$

Let $A_{2^j} f(u, v)$ be the angle of the gradient direction vector (Eq. (2)) in the plane (x, y)

$$A_{2^j} f(u,v) = \tan^{-1}\left(\frac{W_{2^j}^2 f(u,v)}{W_{2^j}^1 f(u,v)}\right). \quad (3)$$

An edge point at the scale 2^j is a point γ such that $M_{2^j} f(u, v)$ is local maximum at $(u = u_\gamma, v = v_\gamma)$ when $\left(u = u + \lambda \vec{n}_j(u_\gamma), v = v + \lambda \vec{n}_j(v_\gamma)\right)$ for $|\lambda|$ small enough. These points are also called WT modulus maxima. A simple criterion is used to detect edges. To capture the spatial details of an image, it is advantageous to make use of a multi-scale representation. In the paper, we extract the angle of the gradient direction of the WT as the iris feature and encode it efficiently. First, we apply WT on the iris image and compute the angle of the gradient direction at a specific scale. In this paper, we use quadratic spline function as the wavelet function.

Individual wavelet modulus maxima are chained together to form a curve that follows an edge. At any location, the tangent of the edge curve is approximated by computing the tangent of the angle of the gradient direction [8]. Thus, we select the angle of the gradient

direction as the iris feature for recognition. It is advantageous because the gradient direction will not be affected by contrast and illumination of the input images. Since singularities and irreguar structures in iris images often carry essential information, we adopt two different representations to extract and encode the features from a human iris image.

3.2. The GDC Method: Gradient Direction Coding with Gray code

The first method, called the GDC method, is gray coding that is a 2-D method and encodes the gradient direction of each small 2-D iris image block in WT domain. The scale of the wavelet representation in this method is $j=4$. Fig. 3 shows the flowchart of the GDC method.
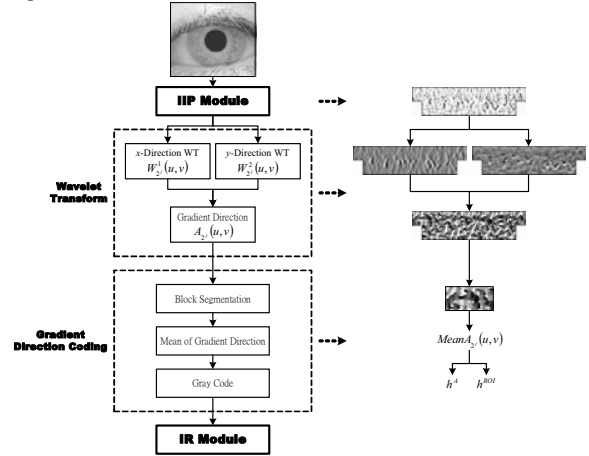

Fig. 3. The flowchart of the GDC method.

After demarcating the iris zone which contains two rectangles with the size 256×32 pixels and two rectangles with the size 212×32 pixels, we subdivide the four 2-D rectangular iris images in the WT gradient direction domain equally into 472 small blocks. The mean of $A_{2^j} f(u,v)$ of all pixels within each iris block is extracted as the edge feature of the block. Accordingly, 472 features for each input iris image are obtained. To reduce the code length of iris features and avoid affected by noise, we encode these features using the Gray code. The codes corresponding to the adjacent intervals differ from only one bit, thus the Hamming distance between them is minimum. On the other hand, the codes corresponding to the interval which differ 180° are different by all of the four bits, thus the Hamming distance between them is maximum. Which code is used to represent the block depends on which interval the mean gradient direction computed from each block belongs to. Totally, a code vector of 295 bytes (including 59 bytes of ROI side information) is generated to represent an iris image by using the GDC method.

3.3. The DMC Method: Delta Modulation Coding

The second method is called the DMC method in which the delta modulation concept is used to efficiently encode the feature information. This is a 1-D method in

which the 2-D feature information is converted into 1-D feature signals before encoding. The encoding method used here is delta modulation. The single bit, providing for just two possibilities ±Δ, is used to increase or decrease the estimated signals. Here, we adopt linear delta modulation (DM) and constant factor adaptive delta modulation (CFDM) in the IFE module.
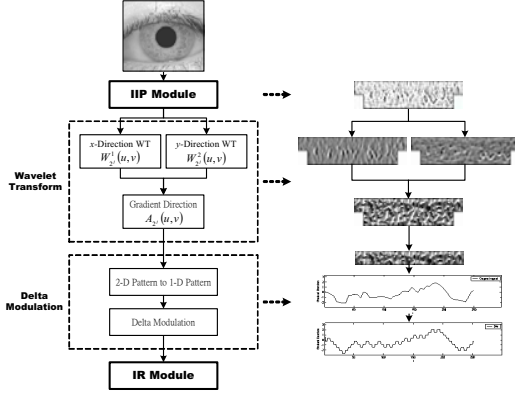

Fig. 4. The flowchart of the DMC method.

In this method, we also use the information of gradient direction in the WT domain at a specific scale for recognition. The scale of the wavelet representation in this method is j=3. Fig. 4 shows the flowchart of this method. We first convert the 2-D iris blocks into 1-D signal with ring-projection by computing the mean of gradient direction of each 8×1 pixels block as a sampled point of the 1-D signal for reducing the dimensionality of 2-D image To acquire shorter code length and outer regions are easily polluted by lower eyelid and eyelashes; and further, the perpendicular texture of iris has more information entropy, we only select the two inner regions of size 256×16, which are closer to pupil, as the iris features. Because of the conversion of 8 vertically consecutive pixels to a sampled point, we obtain four 1-D discrete signals each with the length of 256 points. Totally, there are 1,024 feature points.

After generating four 1-D patterns, we encode each of the patterns by the DM and CFDM methods. If encoding the features with the DM method, we initially select a step size Δ=24 and use sampling rate 1 Hz. With the CFDM method, the step size is set as Δ=16 and the same sampling rate as in the DM method is used. Furthermore, the adaptation logic used in the CFDM method is {M_1=0.7, M_2=0.9, M_3=1.1, M_1=1.4}. As a result, a code vector of 132 bytes is required to represent an iris image with the DM and CFDM coding methods.

3.4. Recognition Module

In this module, the feature code vector extracted from the claimant iris image is compared against those of the enrolled feature code vectors in an iris database we created. Here for simplicity, we adopt the mean vector as the prototype of each pattern class in the enrollment phase and utilize the minimum distance classifier to check the approach in the recognition phase. When the feature code vector in the GDC method is compared, we calculate the normalized Hamming distance HD between two feature code vectors h_1 and h_2, defined as

$$HD(h_1,h_2)=\min_{rad}\frac{\sum_{k}^{K}\sum_{l=0}^{L}\left(h_1^A(k-rad,l)\oplus h_2^A(k,l)\right)\times h_1^{ROI}(k-rad,l)\times h_2^{ROI}(k,l)}{\sum_{k}^{K}\sum_{l}^{L}h_1^{ROI}(k-rad,l)\times h_2^{ROI}(k,l)}$$

where the subscripts k, l denote indexing bit position, $\oplus$ denotes the exclusive-OR operator, and rad denotes correcting the rotation effect of the input iris image. On the other hand, we adopt another metric for the DM and CFDM methods to calculate the normalized Euclidean distance D of feature vectors g_1 and g_2, defined as

$$D(g_1,g_2)=\frac{1}{255\cdot N}\min_{rad}\left(\sum_{m=1}^{N}\left(g_1(m+rad)-g_2(m)\right)^2\right)^{\frac{1}{2}}, D\in[0,1],$$

where m denotes the position of restructured signal and rad correcting the rotation effect of the input iris image.

4. EXPERIMENTAL RESULTS

We implemented and tested the proposed schemes on the CASIA iris image database [6]. It comprises 756 iris images captured from 108 different eyes (hence 108 classes). Each original iris image has the resolution of 320×280 in gray level. For each eye, seven images are captured in two sessions, in which three samples are collected in the first session and four in the second session. Here, False Acceptance Rate (FAR), False Rejection Rate (FRR) and Equal Error Rate (EER) are used to evaluate the performance.

4.1. Results of Image Pre-processing

We check the accuracy of the boundaries (including pupil, iris, and lower eyelid) subjectively and the proposed system obtains the success rate of 82.54% (624 images) from 756 images in the experiments for the pre-processing module. Table 1 shows the summary of the causes of failure of image pre-processing. It is worth noting that the two main causes of failure come from occlusion by eyelids and non-uniform illumination.

Table 1 Analysis of causes of failure for IIP module.

	Causes of Failure	# of Data	Ratio (%)
(1)	Occlusion by eyelids or eyelashes	51	38.64
(2)	Inappropriate eye positioning	2	1.52
(3)	Pupil or iris is not a circular form	2	1.52
(4)	Non-uniform illumination	71	53.79
(5)	Affected by iris texture	3	2.27
(6)	etc.	3	2.27
Total		132	100

Among those 624 images obtained successfully from the image pre-processing module, we select 587 images (90 classes) out of them for testing (enrollment and recognition). A half of 90 classes are regarded as legal users and the rest as impostors (illegal users). We train the system by selecting 3 images as the training image set for each person from the authorized users in the enrollment phase. Hence, there are 317 images for testing (160 images from the authorized users and 157 images from the impostors).

4.2. Results of the GDC Method

We perform two tests: one is for false rejection test (160 images) and the other is for false acceptance rate test (157 images). For the case of FRR, we can obtain the distribution of non-matching distance between the unknown classes and the registered classes. For the case of FAR, we also obtain the distribution of non-matching between the unknown classes for impostors and the registered classes. Fig. 5(a) shows the distributions of the above two experiments. Fig. 5(b) shows the plot of variation of FRR and FAR according to the distribution of non-matching distance by selecting a proper distance threshold. When we set the threshold to be 0.3775, the system obtains the recognition performance of about EER=4.73%. And when the FAR is set to be 0%, the system can obtain FRR=6.88% at a threshold of 0.36. In particular, if we use a code vector of 585 bytes instead of 295 bytes, the recognition performance of the proposed system can be lower to 0.95% only. The experimental results show that the proposed system performs well.
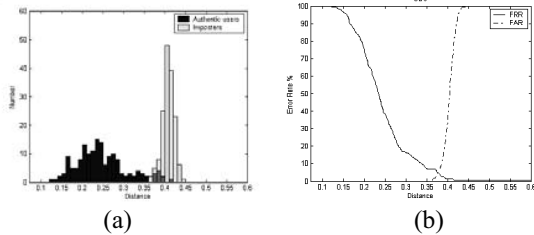

| (a) | (b) |

Fig. 5. The GDC method: (a) the distribution of non-matching distance, (b) variation of FRR and FAR.

4.3. Results of the DMC Method

In the DM method, we obtain the distribution of non-matching distance for FRR and FAR experiments, as shown in Fig. 6(a). Fig. 6(b) shows the plot of variation of FRR and FAR by selecting a proper distance threshold. By selecting the threshold of 0.1785, the system obtains the system performance of EER=4.38%. Similarly, if the FAR is set to be 0%, the system can obtain FRR=9.38% at a threshold of 0.173.

Next, we perform the same experiments for the CFDM method. The distribution of non-matching distance is shown in Fig. 7(a). Fig. 7(b) shows the plot of variation of FRR and FAR. The system performance is about EER=3.79% by selecting the threshold of 0.1645. Similarly, if FAR is set to be 0%, the system can obtain FRR=8.13% at a threshold of 0.159. The results show that the CFDM method performs better slightly than the DM method. The superiority of the CFDM method should come from the fact that it is adaptive.

Table 2 shows the comparison of identification performances. It can be seen that both the DM and CFDM methods have a superior performance to the GDC method by comparing the EER performance. On the other hand, the DM method can performs superiorly in the case of FAR=0%. Consequently, the GDC method provides a securer system than the DM methods.
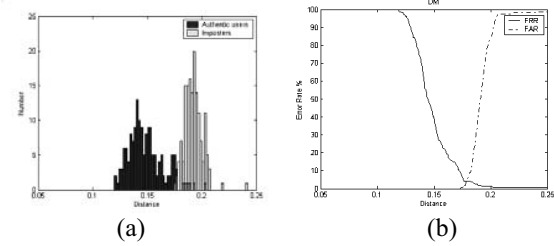

| (a) | (b) |

Fig. 6. The results of the DM method.

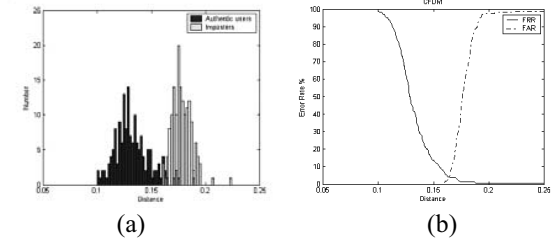| (a) | (b) |

Fig. 7. The results of the CFDM method.

Table 2 Comparison of identification performance.

Mode	IFE Module	Size of Features	RA (%)	AA (%)	AF (%)	RF (%)
ERR	GDC	585 bytes	0.95	99.05	0.95	99.05
	GDC	295 bytes	4.73	95.27	4.73	95.27
	GDC	147 bytes	5.94	94.06	5.94	94.06
	DM	132 bytes	4.38	95.62	4.38	95.62
	CFDM	132 bytes	3.79	96.21	3.79	96.21
FAR = 0%	GDC	295 bytes	6.88	93.12	0	100
	GDC	147 bytes	7.50	92.50	0	100
	DM	132 bytes	9.38	90.62	0	100
	CFDM	132 bytes	8.13	91.87	0	100

5. REFERENCES

[1] A. K. Jain, R. Bolle and S. Pankanti, *Biometrics: Personal Identification in Network Society*. Kluwer Academic Publishers, 1999.

[2] J. G. Daugman, "High confidence visual recognition of persons by a test of statistical independence," *IEEE Trans. Patt. Analy. & Mach. Intell.*, vol. 15, No. 11, pp. 1148-1161, Nov. 1993.

[3] R. P. Wildes, *et al.*, "A machine-vision system for iris recognition," *Machine Vision and Applications*, Springer-Verlag, 1996.

[4] W. W. Boles and B. Boashash, "A human identification technique using images of the iris and wavelet transform," *IEEE Trans. Signal Proc.*, vol. 46, No. 4, pp. 1185-1188, Apr. 1998.

[5] L. Ma, T. Tan, Y. Wang and D. Zhang, "Personal identification based on iris texture analysis," *IEEE Trans. Patt. Analy. & Mach. Intell.*, vol. 25, No. 12, pp. 1519-1533, Dec. 2003.

[6] Institute of Automation, Chinese Academy of Sciences, *CASIA Iris Image Database*, http://www.sinobiometrics.com/.

[7] Y. Y. Tang, *et al.*, *Wavelet Theory and Its Application to Pattern Recognition*, World Scientific, Singapore, 2000.